On the $\mathcal{O}(1)$ Solution of Multiple-Scattering Problems

Christophe Geuzaine[1,3], *Member, IEEE*, Oscar Bruno[1], and Fernando Reitich[2]

[1]California Institute of Technology, Department of Applied and Computational Mathematics, Pasadena, CA 91125 USA
[2] University of Minnesota, School of Mathematics, Minneapolis, MN 55455, USA
[3]Belgian National Fund for Scientific Research (FNRS), University of Liège, B-4000 Liège, Belgium

In this paper, we present a multiple-scattering solver for nonconvex geometries such as those obtained as the union of a finite number of convex surfaces. For a prescribed error tolerance, this algorithm exhibits a *fixed computational cost for arbitrarily high frequencies*. At the core of the method is an extension of the method of stationary phase, together with the use of an ansatz for the unknown density in a combined-field boundary integral formulation.

***Index Terms*—Wave scattering, boundary integral equations, spectral methods, high-frequency methods.**

I. Introduction

CURRENT state-of-the-art simulation technology for high-frequency scattering relies on methods that are based on approximations of Maxwell's equations, such as the geometrical theory of diffraction [1]. These methods are not error-controllable, since the most accurate solution they can produce exhibits an error on the order of the wavelength. A most attractive feature of these procedures, however, is that they can bypass the resolution of the wavelength and work with frequency-independent discretizations. An "ideal" solver for the high-frequency regime then would be one that retains this feature without compromising error-controllability.

Our recent work [2] (see also [3] and [4]) has demonstrated the feasibility of such an $\mathcal{O}(1)$ numerical scheme for surface-scattering problems by *convex* obstacles. This algorithm evaluates scattering at arbitrarily high-frequencies, with a prescribed accuracy, and in a frequency-independent (thus $\mathcal{O}(1)$) computational time. Further, this method exhibits high-order convergence, which minimizes the computational effort to achieve a given error.

In the present paper, after a short review of the algorithm proposed in [2], we discuss extensions that are needed to deal with certain types of *nonconvex* geometries. In particular, we show that each one of the multiple reflections that arise in the multiple-scattering configurations considered presently can be evaluated by means of the single-scattering methods of [2].

For simplicity we restrict ourselves to the evaluation of the scattering of a plane wave $u^{\rm inc}(\boldsymbol{r}) = e^{ik\boldsymbol{\alpha}\cdot\boldsymbol{r}}$, $|\boldsymbol{\alpha}| = 1$, on an impenetrable obstacle D in two dimensions (a TE-electromagnetic problem). In this context, if $\partial D = S$ denotes the boundary of D, the relevant frequency-domain problem is modeled by the scalar combined-field integral equation formulation

$$\frac{1}{2}\mu(\boldsymbol{r}) - \int_S H(\boldsymbol{r},\boldsymbol{r}')\mu(\boldsymbol{r}')\,ds(\boldsymbol{r}') = \frac{\partial u^{\rm inc}(\boldsymbol{r})}{\partial \boldsymbol{\nu}(\boldsymbol{r})} + i\gamma u^{\rm inc}(\boldsymbol{r}), \qquad \boldsymbol{r}\in S \quad (1)$$

with

$$H(\boldsymbol{r},\boldsymbol{r}') = \frac{\partial \Phi(\boldsymbol{r},\boldsymbol{r}')}{\partial \boldsymbol{\nu}(\boldsymbol{r})} + i\gamma\Phi(\boldsymbol{r},\boldsymbol{r}').$$

In this formulation, $\mu(\boldsymbol{r}) = \partial u(\boldsymbol{r})/\partial\boldsymbol{\nu}(\boldsymbol{r})$ denotes the current, $\boldsymbol{\nu}(\boldsymbol{r})$ is the outward unit normal to S at point $\boldsymbol{r}$, $\Phi(\boldsymbol{r},\boldsymbol{r}')$ is the radiating free-space Green function, and γ is a coupling constant.

II. Single Scattering

A. Ansatz for the Current

For single-scattering configurations (which arise, e.g., when D is convex), our method of solution of (1) is based on the observation that, away from shadow regions, the unknown current $\mu(\boldsymbol{r})$ oscillates like the incoming radiation [5], [6], that is,

$$\mu(\boldsymbol{r}) = \mu_{\rm slow}(\boldsymbol{r})e^{ik\boldsymbol{\alpha}\cdot\boldsymbol{r}}. \quad (2)$$

It follows that (1) can be rewritten as

$$\frac{1}{2}\mu_{\rm slow}(\boldsymbol{r}) - \int_S H(\boldsymbol{r},\boldsymbol{r}')e^{ik[\varphi^0(\boldsymbol{r}')-\varphi^0(\boldsymbol{r})]}\mu_{\rm slow}(\boldsymbol{r}')\,ds(\boldsymbol{r}') = g^0_{\rm slow}(\boldsymbol{r}), \quad \boldsymbol{r}\in S \quad (3)$$

with

$$\varphi^0(\boldsymbol{r}) = \boldsymbol{\alpha}\cdot\boldsymbol{r} \quad \text{and} \quad g^0_{\rm slow}(\boldsymbol{r}) = i(k\boldsymbol{\alpha}\cdot\boldsymbol{\nu}(\boldsymbol{r}) + \gamma).$$

Throughout the illuminated region of S, the variations in the envelope $\mu_{\rm slow}$ in (3) *do not* accentuate with increasing frequency and thus, for arbitrarily short wavelengths, $\mu_{\rm slow}$ can be represented, to any prescribed accuracy, with a *fixed* number of discretization points [2].

In an effort to produce an algorithm that can solve (1) with fixed accuracy and with a frequency-independent computational cost, the following two main challenges arise.

1) The ansatz of (2) is not valid in the vicinity of shadow boundaries (where $\boldsymbol{\alpha}\cdot\boldsymbol{\nu}(\boldsymbol{r}) = 0$).
2) Even if $\mu_{\rm slow}$ could be represented with a fixed number of degrees of freedom, the numerical evaluation of the integrals in (3) would require a number of quadrature points

Digital Object Identifier 10.1109/TMAG.2005.844567

large enough to resolve the wavelength, leading to a computational complexity that increases with frequency.

As we have shown in [2], the first problem can be overcome by using frequency-dependent changes of variables within the boundary layers around the shadow boundaries where the ansatz (2) breaks down. Beyond these boundary layers and toward the illuminated region the ansatz holds true, while toward the deep shadow the current vanishes exponentially and its contribution to the integral can be controllably neglected. Moreover, the oscillations in μ_{slow} within the boundary layer occur precisely on the lengthscale of the transition region and, therefore, the current there can again be resolved with a *fixed* number of discretization points.

To solve the second problem, as is explained next, we use a localized integration scheme around the critical points of the oscillatory integral in (3).

B. Stationary Phase and Localized Integration

For a sufficiently large wavenumber k and for $\boldsymbol{r} \neq \boldsymbol{r}'$ the kernel $H(\boldsymbol{r},\boldsymbol{r}')e^{ik[\varphi^0(\boldsymbol{r}')-\varphi^0(\boldsymbol{r})]}$ behaves like the kernel

$$e^{ik\left[|\boldsymbol{r}-\boldsymbol{r}'|+\varphi^0(\boldsymbol{r}')-\varphi^0(\boldsymbol{r})\right]} \equiv e^{ik\phi}$$

of a generalized Fourier integral. It follows that, *asymptotically*, the only significant contributions to the oscillatory integral in (3) arise from values of μ_{slow} and its derivatives at the critical points [7]; in the present context, these critical points are the target point (where the kernel is singular) and the stationary phase points (where the gradient of the phase ϕ vanishes).

In order to obtain a *convergent* (not merely asymptotic) method for *arbitrary frequencies* which runs in *frequency independent* computing times, we introduced the following localized integration procedure *around* the critical points in [2]: For each target point $\boldsymbol{r}$ on the surface S, the corresponding set of critical points is covered by a number of small regions:

1) the target point is covered by a region of radius proportional to the wavelength $\lambda = 2\pi/k$;
2) the ℓth stationary phase point is covered by a region of radius proportional to $\sqrt[3]{\lambda}$ (at the shadow boundaries) or $\sqrt{\lambda}$ (away from the shadow boundaries).

A partition of unity [8] is then used to reduce the integral over S into a number of integrals over these small regions, each of which can be evaluated numerically to high order using appropriate quadrature rules [2]. In practice, this localized integration method can be thought of as an error-controllable version of the "asymptotic method of stationary phase" [7].

Since the density μ_{slow} can be represented with a fixed number of degrees of freedom for arbitrary k and since the size of the regions associated with the critical points shrinks as the frequency increases (so that the number of oscillations of the integrand in each interval remains constant), the overall procedure results, as desired, in a convergent integration method whose computational complexity is independent of frequency. The numerical method is then completed through use of the iterative linear algebra solver GMRES.

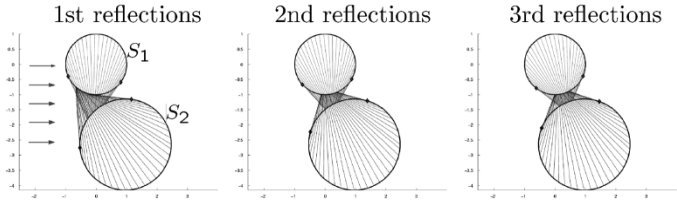

Fig. 1. Geometrical optics solution for a configuration of two circular cylinders S_1 and S_2, with radii $r_1 = 1,\ r_2 = 1.5$.

III. Multiple Scattering

The extension of our method to multiple-scattering configurations is based on three main elements:

1) an iteratively computable Neumann series for the currents induced on the scattering surfaces, which accounts rigorously for multiple scattering;
2) a generalized ansatz that allows for *a priori* determination of the highly oscillatory phase of the currents in each term of the series; and
3) use of the single-scattering algorithm mentioned above for the $\mathcal{O}(1)$ evaluation of each one of the terms in this series.

A. Neumann Series for Multiple Reflections

Let us consider a surface $S = S_1 \cup S_2$ composed of two convex, closed subsurfaces S_1 and S_2 (see, e.g., Fig. 1). In this case (1) takes on the form

$$\frac{1}{2}\mu_i(\boldsymbol{r}) - \sum_{j=1}^{2}\int_{S_j} H(\boldsymbol{r},\boldsymbol{r}')\mu_j(\boldsymbol{r}')\,ds(\boldsymbol{r}') = g^0_{i,\text{slow}}(\boldsymbol{r})e^{ik\varphi^0_i(\boldsymbol{r})}, \qquad \boldsymbol{r}\in S_i, \quad i=1,2,$$

where $\mu(\boldsymbol{r}) \equiv \mu_i(\boldsymbol{r}), \varphi^0(\boldsymbol{r}) \equiv \varphi^0_i(\boldsymbol{r})$, and $g^0_{\text{slow}}(\boldsymbol{r}) \equiv g^0_{i,\text{slow}}(\boldsymbol{r})$ in S_i. Alternatively, this equation can be written as

$$(I-B)\begin{bmatrix}\mu_1\\ \mu_2\end{bmatrix} = \begin{bmatrix}2g^0_{1,\text{slow}}(\boldsymbol{r})e^{ik\varphi^0_1(\boldsymbol{r})}\\ 2g^0_{2,\text{slow}}(\boldsymbol{r})e^{ik\varphi^0_2(\boldsymbol{r})}\end{bmatrix} \tag{4}$$

where

$$B = \begin{bmatrix}T_{11} & R_{12}\\ R_{21} & T_{22}\end{bmatrix}$$

and the operators T_{ii} and R_{ij} are defined as

$$T_{ii}(\mu_i)(\boldsymbol{r}) = 2\int_{S_i} H(\boldsymbol{r},\boldsymbol{r}')\mu_i(\boldsymbol{r}')\,ds(\boldsymbol{r}'), \quad \boldsymbol{r}\in S_i$$
$$R_{ij}(\mu_j)(\boldsymbol{r}) = 2\int_{S_j} H(\boldsymbol{r},\boldsymbol{r}')\mu_j(\boldsymbol{r}')\,ds(\boldsymbol{r}'), \quad \boldsymbol{r}\in S_i.$$

The operators in the diagonal of the matrix B correspond precisely to the scattering problems for each isolated subsurface and are therefore invertible. Thus, (4) is equivalent to

$$(I-A)\begin{bmatrix}\mu_1\\ \mu_2\end{bmatrix} = \begin{bmatrix}[I-T_{11}]^{-1}2g^0_{1,\text{slow}}(\boldsymbol{r})e^{ik\varphi^0_1(\boldsymbol{r})}\\ [I-T_{22}]^{-1}2g^0_{2,\text{slow}}(\boldsymbol{r})e^{ik\varphi^0_2(\boldsymbol{r})}\end{bmatrix} \tag{5}$$

with

$$A = \begin{bmatrix}0 & [I-T_{11}]^{-1}R_{12}\\ [I-T_{22}]^{-1}R_{21} & 0\end{bmatrix}.$$

The series solution of (5) is given by

$$\begin{bmatrix}\mu_1\\ \mu_2\end{bmatrix} = \sum_{m=0}^{\infty}\begin{bmatrix}\mu_1^m\\ \mu_2^m\end{bmatrix} \tag{6}$$

where the terms are inductively defined as

$$\begin{bmatrix}\mu_1^0\\ \mu_2^0\end{bmatrix} = \begin{bmatrix}[I-T_{11}]^{-1}2g_{1,\mathrm{slow}}^0(\boldsymbol{r})e^{ik\varphi_1^0(\boldsymbol{r})}\\ [I-T_{22}]^{-1}2g_{2,\mathrm{slow}}^0(\boldsymbol{r})e^{ik\varphi_2^0(\boldsymbol{r})}\end{bmatrix} \tag{7}$$

and

$$\begin{bmatrix}\mu_1^m\\ \mu_2^m\end{bmatrix} = A\begin{bmatrix}\mu_1^{m-1}\\ \mu_2^{m-1}\end{bmatrix}, \quad m\geq 1. \tag{8}$$

More explicitly, relations (7) and (8) can be expressed as

$$\frac{1}{2}\mu_i^0(\boldsymbol{r}) - \int_{S_i} H(\boldsymbol{r},\boldsymbol{r}')\mu_i^0(\boldsymbol{r}')\,ds(\boldsymbol{r}') = g_{i,\mathrm{slow}}^0(\boldsymbol{r})e^{ik\varphi_i^0(\boldsymbol{r})}, \quad \boldsymbol{r}\in S_i, \quad i=1,2 \tag{9}$$

and

$$\frac{1}{2}\mu_i^m(\boldsymbol{r}) - \int_{S_i} H(\boldsymbol{r},\boldsymbol{r}')\mu_i^m(\boldsymbol{r}')\,ds(\boldsymbol{r}') = \sum_{\substack{j=1\\ j\neq i}}^{2}\int_{S_j} H(\boldsymbol{r},\boldsymbol{r}')\mu_j^{m-1}(\boldsymbol{r}')\,ds(\boldsymbol{r}'), \quad m\geq 1, \quad \boldsymbol{r}\in S_i, \quad i=1,2 \tag{10}$$

respectively.

From (9) and (10), we see that the mth order correction (μ_1^m,μ_2^m) in (6) corresponds precisely to the current generated on each subsurface by the mth order reflection—that is, by the field produced on the subsurface after m bounces of the original incident plane wave. Indeed, on the one hand, (9) corresponds to the solution of the scattering problems for each isolated subsurface in response to the incoming radiation, ignoring interactions. On the other hand, the right-hand side of (10) is precisely the field scattered by each subsurface at the $(m-1)$-st stage, evaluated on the complementary part of the structure. Each one of the problems (9) and (10) can be tackled by means of the methods described in Section II; to do this, however, and in order to derive a representation analogous to (2), we must first identify, as shown in the following section, the phase of each one of the subsequent corrections (μ_1^m,μ_2^m).

B. Generalized Ansatz for the Current

To produce the phase of each correction to the current we appeal to the interpretation of the corrections as corresponding to successive wave reflections—which suggests that the phases must coincide with those arising in a geometrical optics solution.

More precisely, the geometrical optics solution provides a sequence of functions $\delta_i^m(\boldsymbol{r})$ measuring the optical distance traveled by a ray arriving at $\boldsymbol{r}\in S_i$ after m reflections. The overall phase is then defined as

$$\varphi_i^m(\boldsymbol{r}) = \begin{cases}\varphi_i^0(\boldsymbol{r}) = \boldsymbol{\alpha}\cdot\boldsymbol{r}, & m=0,\ \boldsymbol{r}\in S_i\\ \varphi_i^0(\boldsymbol{r}) + \delta_i^m(\boldsymbol{r}), & m\geq 1,\ \boldsymbol{r}\in S_i.\end{cases} \tag{11}$$

(See Fig. 1 for an example.) Using (11), (9)–(10) read

$$\frac{1}{2}\mu_{i,\mathrm{slow}}^m(\boldsymbol{r}) - \int_{S_i} H(\boldsymbol{r},\boldsymbol{r}')e^{ik(\varphi_i^m(\boldsymbol{r}')-\varphi_i^m(\boldsymbol{r}))}\mu_{i,\mathrm{slow}}^m(\boldsymbol{r}')\,ds(\boldsymbol{r}') = g_{i,\mathrm{slow}}^m(\boldsymbol{r}), \quad m\geq 0, \quad \boldsymbol{r}\in S_i, \quad i=1,2 \tag{12}$$

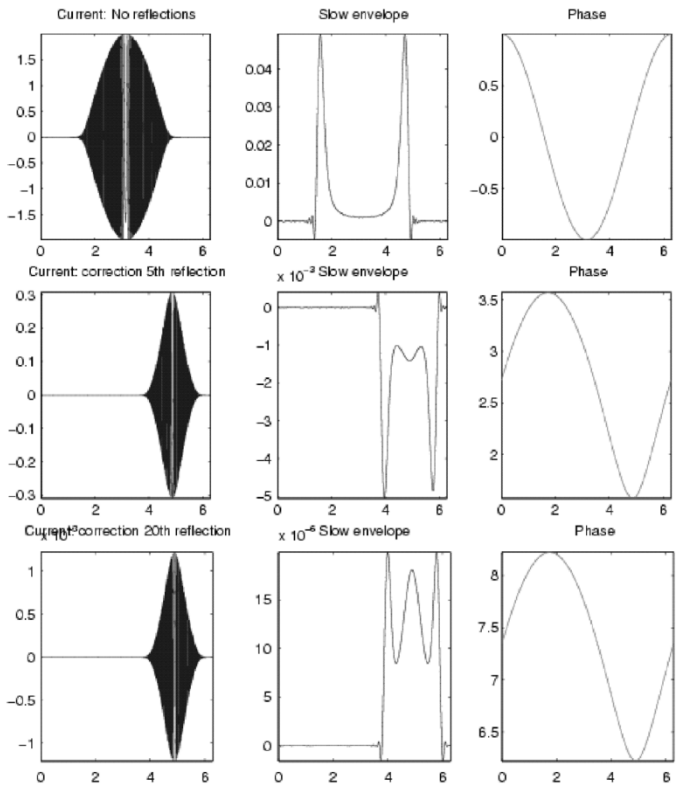

Fig. 2. Slow densities and phases at the first, fifth, and twentieth reflection.

where

$$g_{i,\mathrm{slow}}^m(\boldsymbol{r}) = \begin{cases} i(k\boldsymbol{\alpha}\cdot\boldsymbol{\nu}(\boldsymbol{r})+\gamma), & m=0\\ e^{-ik\varphi_i^m(\boldsymbol{r})}\sum_{\substack{j=1\\ j\neq i}}^{2}\int_{S_j} H(\boldsymbol{r},\boldsymbol{r}')e^{ik\varphi_j^{m-1}(\boldsymbol{r}')} & \\ \mu_{j,\mathrm{slow}}^{m-1}(\boldsymbol{r}')\,ds(\boldsymbol{r}'), & m\geq 1.\end{cases}$$

As we said, the slowly oscillatory character of the latter quantities follows from the interpretation of the right-hand side of (10) as the field scattered by S_i *after* $(m-1)$ reflections, so that its phase is precisely given by $\varphi_i^m(\boldsymbol{r})$. Equation (12) is then amenable to the treatment described in Section II—the only difference being that the evaluation of the right hand side of (12), for $m\geq 1$, entails an integral of a highly oscillatory function. This, however, can again be treated with the aforementioned strategies of localized integration. In fact, in this case the integrand is regular and only integrations around stationary points of the overall phase must be performed. Moreover, as is to be expected from the asymptotic limit, for any given target point $\boldsymbol{r}\in S_i$ there will be exactly one stationary point $\boldsymbol{r}'\in S\setminus S_i$ of the corresponding integral. Indeed, this point will coincide with the point in $S\setminus S_i$ from which a geometrical ray that has experienced $(m-1)$ reflections goes through $\boldsymbol{r}$ upon an additional reflection at $\boldsymbol{r}'$.

C. Numerical Tests

In Figs. 2 and 3, we exemplify our procedure in the specific instance of Fig. 1, i.e., with a scatterer composed of two circular subsurfaces S_1 and S_2. The wavenumber is $k=1000$, so that there are 1000 and 1500 wave oscillations in the perimeter of S_1 and S_2 respectively. In Fig. 2, we display the graphs of the

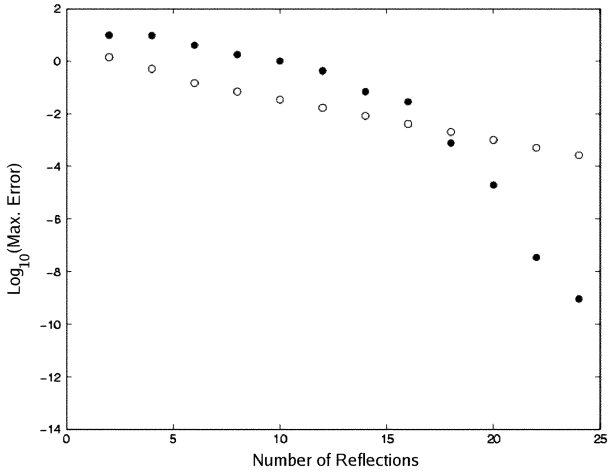

Fig. 3. Error as a function of the number of reflections for $k = 1000$, by direct summation of the series (hollow circles) and by using Padé approximants (filled circles).

functions $\varphi_1^m(\boldsymbol{r})$ and the real parts of the functions $\mu_1^m(\boldsymbol{r})$ and $\mu_{1,\text{slow}}^m(\boldsymbol{r})$ (left, middle, and right panels, respectively) for different values of m ($m = 0, 5, 20$ in the first, second and third rows, respectively). In particular, the figure demonstrates the slowly oscillatory character of the envelopes that result from the generalized phase extraction described above. Indeed, the figure shows that the functions $\mu_{1,\text{slow}}^m(\boldsymbol{r})$ are slowly oscillatory throughout the region of S_1 that is illuminated after m reflections, that they vanish in the corresponding deep shadow zones, and that they exhibit sharp transitions (of the order of $k^{-1/3}$) about shadow boundaries, exactly as in the single-scattering case. Finally, Fig. 3 illustrates the convergence properties of the series (6). More precisely, there we display the values of truncated approximations

$$\tilde{\mu}_{1,M}(\boldsymbol{r}) = \frac{1}{k} \sum_{m=0}^{M} \mu_1^m(\boldsymbol{r}) \tag{13}$$

and of the error

$$\text{Max. Error} = \max |\tilde{\mu}_{1,M}(\boldsymbol{r}) - \mu_1(\boldsymbol{r})|/k \tag{14}$$

where $\mu_1(\boldsymbol{r})$ is the solution (converged to machine precision) obtained by means of the algorithm proposed in ([9, p. 66]), and where the error is normalized by the wave number (note that $\max |\mu_1(\boldsymbol{r})/k \approx 2$).

The hollow circles in Fig. 3 demonstrate the spectral rate of convergence of the series, which translates for instance in an error of 1% for $M = 15$. For this particular error constraint, the total computational time required by our approach on a 1.5 GHz PC was of 7.5 min, independently of the wave number (here with $k = 1000$). As a comparison, to obtain the same precision, the computational time for the direct solver from ([9, p. 66]), using GMRES as a linear algebra solver, would be about 2 h for $k = 1000$ and nine days for $k = 10\,000$.

The filled circles in Fig. 3 show how the convergence of the series can be improved even further by analytic continuation using Padé approximants [10]—in this case leading to an error of less than 1.e-9 for $M = 24$.

IV. Conclusion

We have presented an algorithm for the solution of multiple-scattering problems that can deliver error-controllable solutions for arbitrarily high frequencies at a fixed computational cost, and which builds on our previous development of such an approach for single-scattering configurations. We have explicitly discussed multiple reflections between two convex sections of a two-dimensional scattering structure and have illustrated the approach in the particular case of a two-cylinder scatterer with a narrow inter-cylinder separation.

The rather general nature of our considerations makes them clearly extendable to general three-dimensional configurations, with any finite number of interacting parts. Such planned extensions, we expect, will allow for the solution of a variety of scattering problems that are currently out of reach for even the most advanced rigorous solvers.

Acknowledgment

This work was supported in part by the Air Force Office of Scientific Research, the Defense Advanced Research Projects Agency, the Army High Performance Computing Research Center, the National Science Foundation, and the Belgian Science Policy (P5/34).

References

[1] J. B. Keller, "The geometrical theory of diffraction," presented at the Symp. Microwave Optics, Montreal, QC, Canada, 1953.

[2] O. Bruno, C. Geuzaine, J. Monro Jr., and F. Reitich, "Prescribed error tolerances within fixed computational times for scattering problems of arbitrarily high frequency: The convex case," *Philos. Trans. R. Soc. A, Math., Phys., Eng. Sci.*, vol. 362, pp. 629–645, 2004.

[3] O. P. Bruno, "Fast, high-order, high-frequency integral methods for computational acoustics and electromagnetics," in *Topics in Computational Wave Propagation: Direct and Inverse Problems*, ser. Lecture notes in computational science and engineering. New York: Springer-Verlag, 2003, pp. 43–82.

[4] O. Bruno and C. Geuzaine, "A high-order, high-frequency method for surface scattering by convex obstacles," in *Proc. 14th Conf. Computation of Electromagnetic Field (COMPUMAG) 2003*, Saratoga Springs, NY, Jul. 2003, pp. 132–133.

[5] R. M. James, "A contribution to scattering calculation for small wavelengths—The high frequency panel method," *IEEE Trans. Antennas Propagat.*, vol. 38, no. 10, pp. 1625–1630, Oct. 1990.

[6] K. R. Aberegg and A. F. Peterson, "Application of the integral equation-asymptotic phase method to two-dimensional scattering," *IEEE Trans. Antennas Propagat.*, vol. 43, no. 5, pp. 534–537, May 1995.

[7] N. Bleistein and R. A. Handelsman, *Asymptotic Expansions of Integrals*. New York: Dover, 1986.

[8] O. P. Bruno and L. A. Kunyansky, "High-order algorithm for the solution of surface scattering problems: Basic implementation, tests, and applications," *J. Computat. Phys.*, vol. 169, pp. 80–110, 2001.

[9] D. Colton and R. Kress, *Inverse Acoustic and Electromagnetic Scattering Theory*. New York: Springer-Verlag, 1998.

[10] G. A. Baker Jr. and P. Graves-Morris, *Padé Approximants*. Cambridge, U.K.: Cambridge Univ. Press, 1996.

Manuscript received June 8, 2004.